Magnetic and pair correlations of the Hubbard model with next-nearest-neighbor hopping

Alain F. Veilleux, Anne-Marie Daré, Liang Chen, Y. M. Vilk, and A.-M. S. Tremblay
Département de Physique and Centre de Recherche en Physique du Solide,
Université de Sherbrooke, Sherbrooke, Québec, Canada J1K 2R1
(Received 14 July 1995)

A combination of analytical approaches and quantum Monte Carlo simulations is used to study both magnetic and pairing correlations for a version of the Hubbard model that includes second-neighbor hopping $t'=-0.35t$ as a model for high-temperature superconductors. Magnetic properties are analyzed using the two-particle self-consistent approach. The maximum in magnetic susceptibility as a function of doping appears both at finite t' and at $t'=0$ but for two totally different physical reasons. When $t'=0$, it is induced by antiferromagnetic correlations while at $t'=-0.35t$ it is a band structure effect amplified by interactions. Finally, pairing fluctuations are compared with T-matrix results to disentangle the effects of van Hove singularity and of nesting on superconducting correlations. The addition of antiferromagnetic fluctuations increases slightly the d-wave superconducting correlations despite the presence of a van Hove singularity which tends to decrease them in the repulsive model. Some aspects of the phase diagram and some subtleties of finite-size scaling in Monte Carlo simulations, such as inverted finite-size dependence, are also discussed.

I. INTRODUCTION

High-temperature superconductors pose a theoretical challenge[1] for many reasons. One of them is that their band structure does not suffice by itself to explain most experiments, even in the normal state. This is one of the reasons that much work has been devoted to the simplest model which incorporates the effects of short-range interactions, the Hubbard model,

$$H=-\sum_{\langle ij\rangle\sigma} t_{i,j}(c^{\dagger}_{i\sigma}c_{j\sigma}+c^{\dagger}_{j\sigma}c_{i\sigma})+U\sum_{i} n_{i\uparrow}n_{i\downarrow}. \quad (1)$$

In this expression, the operator $c_{i\sigma}$ destroys an electron of spin σ at site i. Its adjoint $c^{\dagger}_{i\sigma}$ creates an electron. The symmetric hopping matrix $t_{i,j}$ determines the band structure. We consider the case where $t_{i,j}=t$ for nearest neighbors, $t_{i,j}=t'$ for next-nearest neighbors, and $t_{i,j}=0$ otherwise. Double occupation of a site costs an energy U due to the screened Coulomb interaction. We work in units where the lattice spacing is unity, $k_B=1$, $\hbar=1$, and $t=1$. Since high-temperature superconductivity generally occurs in systems with a pronounced planar structure, the two-dimensional square lattice version of the model is considered, as usual.

The nearest-neighbor ($t'=0$) version of the above Hubbard model has been extensively studied. Within this model, the only hope to get even qualitative agreement with experiment is if the interactions or the antiferromagnetic fluctuations are very strong. Indeed, with the nearest-neighbor model the Fermi surface topology and the filling dependence of both the Hall coefficient and the uniform magnetic susceptibility are all qualitatively wrong, a disagreement that cannot be removed perturbatively. On the other hand, with second nearest-neighbor hopping, the band structure becomes more realistic and all the above physical quantities as well as the position of neutron scattering intensity maxima[2–5] have at least the correct qualitative behavior.

It is thus important to understand the Hubbard model Eq. (1) including both nearest-neighbor hopping t and next-nearest-neighbor hopping t' since weaker interactions in this more realistic model might suffice to explain the experimental data. Two main questions are addressed here by a combination of numerical[6–12] and analytical approaches:[13] First, the origin of the maximum in the uniform magnetic susceptibility as a function of band filling at low temperature, and second, the relative influence of density of state effects (van Hove singularity) and Fermi surface-topology effects (nesting) on pairing correlations. While both van Hove singularity and nesting occur simultaneously at half-filling in the usual $t'=0$ model, there is no nesting when $t'\neq 0$.[14]

In the rest of this paper we first discuss the Monte Carlo approach and the range of parameters studied. In this same section, we discuss subtleties of finite-size scaling including an effect that does not occur in the nearest-neighbor model, namely, inverted finite-size scaling. In the following two sections, we present results in turn for the magnetic susceptibility and for antiferromagnetic as well as pairing correlations along with analytical[15] approaches to understand the results. It will be shown that for magnetic properties, the recently proposed two-particle self-consistent (TPSC) approach[16] compares very well with Monte Carlo results, allowing us to understand the origin of the maximum in magnetic uniform magnetic susceptibility as well as some features of the phase diagram. The same kind of agreement was found before in the case of the nearest-neighbor model.[16] Superconducting fluctuations on the other hand are accounted for by T-matrix effects far from the van Hove singularity.[17,18] The physical interpretation of the results is summarized in the conclusion.

II. QUANTUM MONTE CARLO APPROACH, SIMULATION PARAMETERS, AND FINITE-SIZE EFFECTS

After a brief discussion of technical details of the simulations, we make several general points about finite-size effects. These effects can be especially unusual in the presence

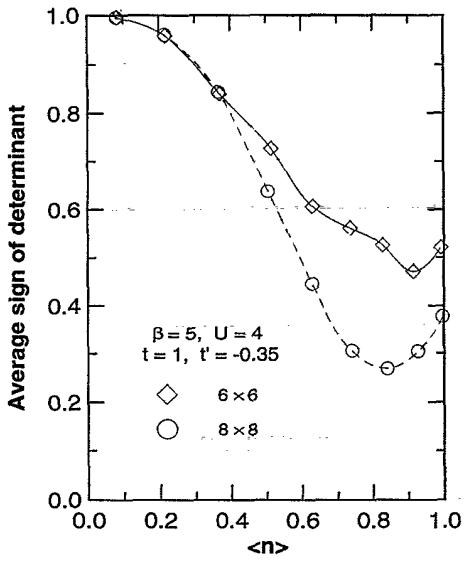

FIG. 1. Average sign of the determinant as a function of filling for the next-nearest-neighbor hopping model.

of t'. We point out in particular how false signals of antiferromagnetism can be detected as an inverse finite-size dependence. Finite-size effects will be discussed further in the other sections for each specific physical situation encountered.

A. Simulations

We use the so-called determinantal quantum Monte Carlo approach.[20–23] As usual the sign of the fermion determinant renders the statistical accuracy very poor in certain regions of parameter space so that long computation times are required. Figure 1, computed using the standard gauge[24] for the Hirsch-Hubbard-Stratonovich transformation, gives the average sign of the fermion determinant for typical parameters considered in the present paper. For $t'=0$, the sign was always positive at half-filling because of particle-hole symmetry[25] but this is no longer the case for $t'\neq 0$.

All the simulations presented below are for either $t'=0$, or $t'=-0.35$ which, in addition to minimizing finite-size effects, as described below, is typical for high-temperature superconductors. Indeed, band-structure calculations[26,27] suggest $t'=-0.16$ for La_2CuO_4 and $t'=-0.45$ for $YBa_2Cu_3O_7$.

Two to five different runs were done for each point with 6×10^5 to 2×10^6 measurements per run. Measurements were grouped into 400 equal-size blocks to estimate the statistical error. Between 10^3 and 10^4 flips per spin in space-time were performed for the warm-up period. Sparse matrix techniques were used for the exponential of the kinetic energy operator.[23] The most difficult points took 300 hours each to be obtained at a computing speed of 26 million floating point operations per second. The imaginary-time discretization step was between 1/8 and 1/16. Some results were also obtained on a Fujitsu supercomputer.

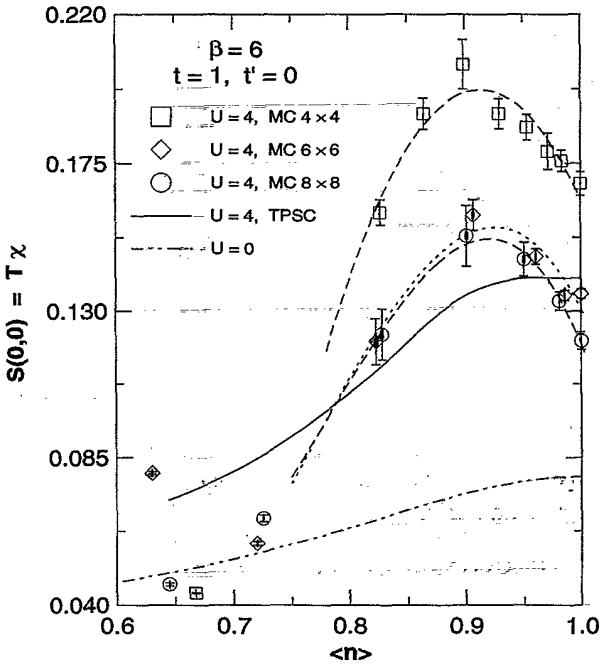

FIG. 2. Maximum in the uniform magnetic susceptibility for the nearest-neighbor model for various system sizes and for the TPSC approach. In the latter case, the calculation is for an infinite system. The curve for 4×4 system is from Ref. 34.

B. Finite-size effects

One should recall that finite-size corrections arise at low temperature because of two different physical effects: (a) the correlation length arising from interaction-induced collective phenomena (antiferromagnetism) can become larger than the system size; (b) the temperature can become smaller than the energy-level separation or, equivalently, the thermal de Broglie wavelength $\xi_{th}=v_F/(\pi T)$ can become larger than the system size. In the latter case, even the results for $U=0$ contain finite-size effects.

Since finite-size effects limit the lowest temperature that we can consider, they also determine the smallest accessible value of the next-nearest-neighbor hopping t'. Indeed, nontrivial effects caused by t' appear only when $t'>T$. Furthermore, it is important to realize that finite-size corrections may depend on filling at fixed temperature. This is particularly important in the context of one of our problems, namely the maximum in the uniform magnetic susceptibility as a function of doping at low temperature. Our results, in Figs. 2 and 3, will be discussed in more detail in the next section. To understand finite-size effects here, we first recall that the uniform magnetic susceptibility of the noninteracting infinite system has a maximum away from half-filling as long as $t'\neq 0$. In a 10×10 system at $U=0$, $\beta=1/T=5$, one can check that this maximum first appears away from half-filling only for t' in the vicinity of -0.35. Smaller values of t' do not even lead to a filling dependence qualitatively similar to that of the infinite system at zero temperature. For $t'=-0.35$, several of the allowed wave vectors of the finite system are close to the Fermi surface at the filling n about 0.6 where the van Hove singularity is located in the infinite-size system. This leads to a better finite-size representation of this singularity. The finite-size effects in the noninteracting 8×8 system illustrated by the dashed line in Fig. 3 lead to the small

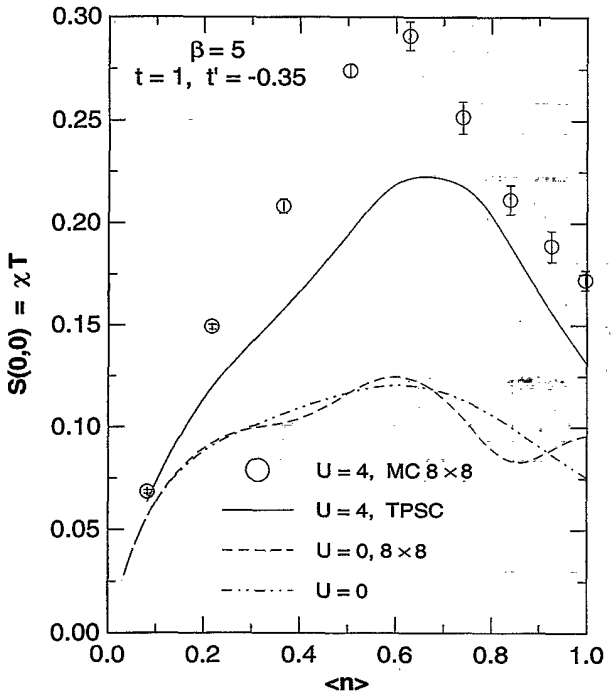

FIG. 3. Maximum in the uniform magnetic susceptibility for the next-nearest-neighbor model for 8×8 system and for the TPSC approach on an infinite lattice. $U=0$ results are also presented for 8×8 and for infinite size to estimate finite-size effects.

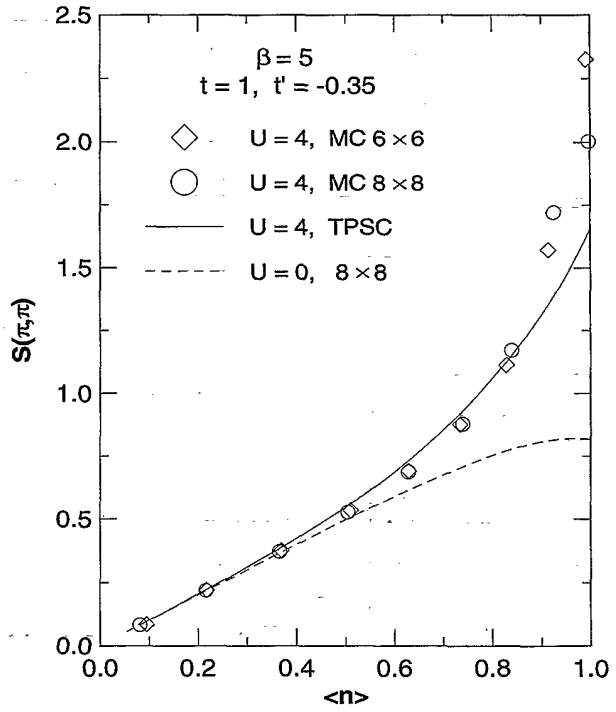

FIG. 4. Magnetic structure factor at the antiferromagnetic wave vector, compared with the TPSC approach in the infinite-size limit. The antiferromagnetic correlation length for the next-nearest-neighbor model is largest at half-filling but remains finite for the parameters considered here.

oscillations around the infinite-size result. These oscillations would become much larger at lower temperature where they could lead to erroneous conclusions.

The interplay between finite-size effects and antiferromagnetic fluctuations in the finite t' model is also very peculiar. Antiferromagnetic fluctuations may be observed in the (π,π) component of the magnetic structure factor defined by

$$S(\mathbf{q})=\frac{1}{N}\sum_{\mathbf{r}_i,\mathbf{r}_j}\exp[i\mathbf{q}\cdot(\mathbf{r}_i-\mathbf{r}_j)]\langle(n_{i,\uparrow}-n_{i,\downarrow})(n_{j,\uparrow}-n_{j,\downarrow})\rangle.$$

Figure 4 allows one to suggest that in the $t'=-0.35$ model the antiferromagnetic fluctuations are largest around $n=1$ since this is where finite-size effects are largest. By contrast with the $t'=0$ model however, we observe here an *inverted finite-size effect*. What we mean is that the magnetic structure factor is converging *down* to the infinite volume result. In the $t'=0$ model, this is never observed. When the correlation length is finite but larger than the system size at this temperature, $S(\mathbf{q})$ normally *increases* with system size until it saturates. The TPSC described below[16] reproduces the inverted finite-size effect of the $t'=-0.35$ model and suggests that Monte Carlo calculations on 10×10 would be necessary to converge to the infinite-size result at this temperature. The source of the inverted finite-size effect can be found already from the $U=0$ calculation which shows that for $t'=-0.35$ the magnitude of the $\mathbf{q}=(\pi,\pi)$ susceptibility on a 6×6 or a 8×8 system is anomalously large compared with the infinite-size limit. This can lead to spurious results in zero-temperature calculations. Indeed, in Ref. 11 it was found that the 6×6, $t'=\pm0.4$ system at half-filling has long-range order at zero temperature. Our analytical TPSC approach suggests that long-range order is present at $T=0$ on both 6×6 and 8×8 systems but not in the infinite volume limit so that the disappearance of long-range order at zero temperature would be apparent, in this case, only for very large systems.

C. Finite-size analytical calculations

The above considerations show that when an analytical approach[15] is available, it can be used to understand finite-size effects by simply comparing the infinite-size limit with calculations on systems that have the same size as those where the simulations are done. It should also be clear that even when an analytical approach is not available, the noninteracting case can carry useful information on spurious finite-size effects that arise when the thermal de Broglie wavelength is larger than the system size. A striking example of this is provided by Fig. 5. At finite temperature ($\beta=5$), the noninteracting susceptibility has qualitatively the same overall magnitude and wave vector dependence on a very large lattice [Fig. 5(a)], and on a small 8×8 lattice [Fig. 5(b)]. In the zero-temperature limit however, Figs. 5(c) and 5(d) show that the 8×8 lattice is qualitatively different from the infinite-lattice result. In particular, on a finite lattice the maximum susceptibility is at zero wave vector and is about five times larger than the true maximum that is furthermore located at a totally different wave vector.

Analytical calculations on finite lattices also have difficulties of their own in the presence of interactions. For example, the random phase approximation (RPA) can be more diver-

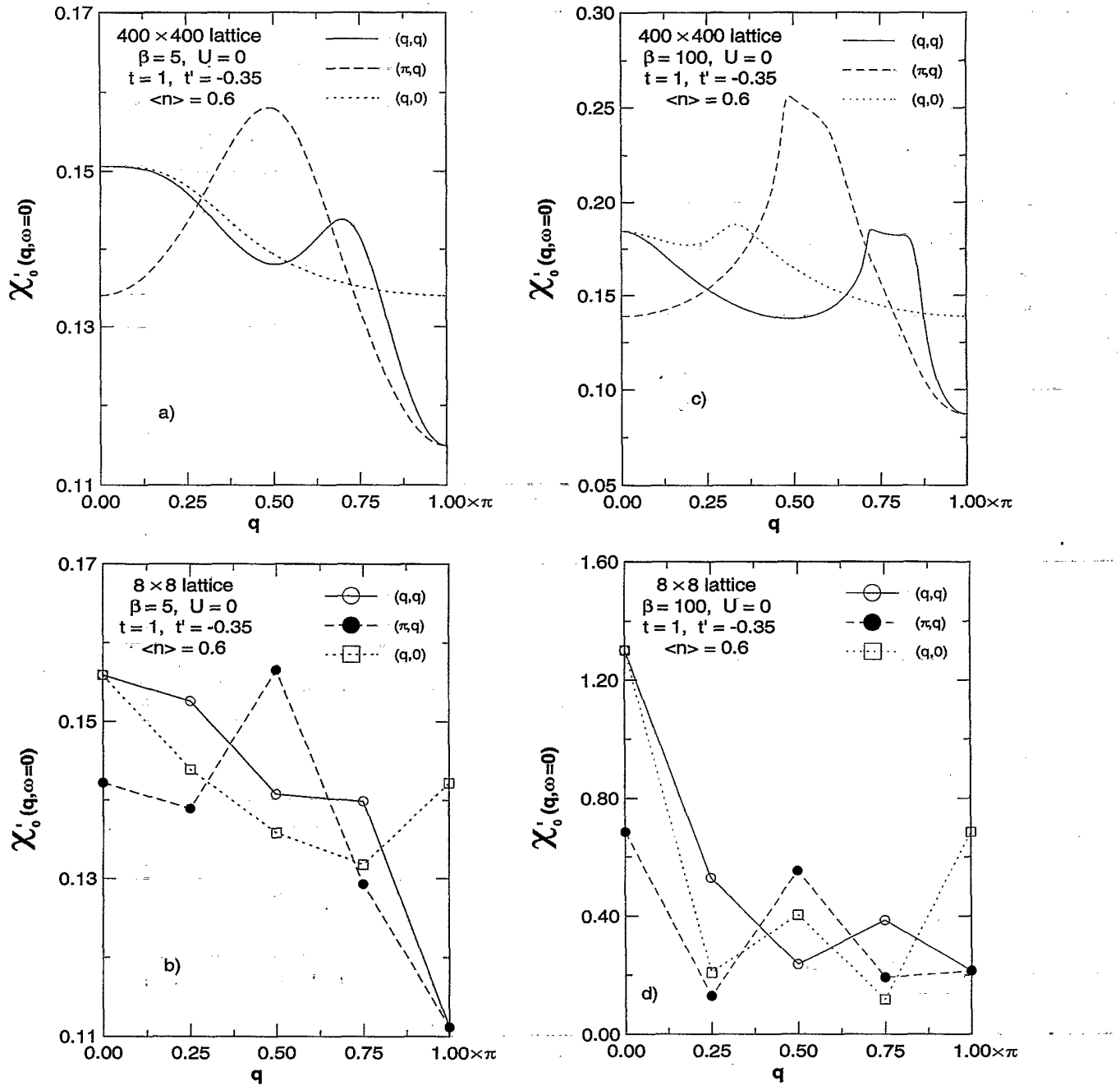

FIG. 5. Finite-size effects in the noninteracting uniform susceptibility when $t'=-0.35$. (a) and (b) calculations are at $\beta=5$ for, respectively, a converged lattice and an 8×8 lattice. (c) and (d) are for the low temperature limit $\beta=100$.

gent on a finite lattice at finite temperature than the corresponding calculation on an infinite lattice. Indeed, consider the Lindhard function

$$\chi_0(\mathbf{q},iq_n=0)=-\frac{1}{N}\sum_{\mathbf{k}}\frac{f(\epsilon_{\mathbf{k}})-f(\epsilon_{\mathbf{k}+\mathbf{q}})}{\epsilon_{\mathbf{k}}-\epsilon_{\mathbf{k}+\mathbf{q}}}, \tag{2}$$

where the sum is over the N discrete lattice points of the Brillouin zone, and $f(\epsilon_{\mathbf{k}})$ is the Fermi function. Suppose that for m of the wave vectors on the Fermi surface, the condition $\epsilon_{\mathbf{k}}=\epsilon_{\mathbf{k}+\mathbf{q}}$ is satisfied. Then the total contribution of these points to the Lindhard function is given by

$$-\frac{m}{N}\frac{\partial f(\epsilon_{\mathbf{k}})}{\partial\epsilon_{\mathbf{k}}}\bigg|_{\epsilon_{\mathbf{k}}=\mu}=\frac{m}{4TN}. \tag{3}$$

On a finite lattice this contribution becomes huge at small temperatures $T\ll m/(4N)$ while it is never the case in the infinite-size $N\to\infty$ limit. Hence the RPA susceptibility $\chi_0/(1-U\chi_0)$ may be divergent on a finite lattice at low temperature, even when for an infinite system the condition $U\chi_0\ll1$ ensuring the validity of RPA is satisfied. Since susceptibilities are always finite on finite systems, this shows that perturbative techniques that are appropriate for infinite

lattices may fail when applied on small systems. In the case just discussed, the infinite-lattice result obtained from RPA may be closer to the true finite-lattice result than the same RPA calculation done on the finite system. Consequently, in the TPSC approach[16] described below, the intermediate quantity $\chi_0(\mathbf{q},iq_n=0)$ appearing in the calculations sometimes has to be computed for a discrete set of $\mathbf{q}$ wave vectors but with a sum over $\mathbf{k}$ done for the infinite system to correctly estimate finite-size effects. Note that when the de Broglie wavelength is smaller than the system size, then the inequality $[\xi_{\rm th}=v_F/(\pi T)]<N^{1/2}$ ensures that the troublesome condition $T\ll m/(4N)$ does not occur since $T>v_F/(\pi N^{1/2})$ generally implies that $T\gg 1/N$ is satisfied.

III. MAGNETIC STRUCTURE FACTOR AND TWO-PARTICLE SELF-CONSISTENT APPROXIMATION

The two-particle self-consistent approximation (TPSC) (Ref. 16) agrees at the few percent level with simulations on the nearest-neighbor model up to intermediate coupling ($U<8$). The agreement is overall better than in the fluctuation exchange approximation FLEX or parquet.[28] While direct diagrammatic approaches[29,30] can work well far from half-filling, they fail as soon as antiferromagnetic fluctuations start to increase. Hence we compare our Monte Carlo results only with the TPSC approach. We first briefly discuss the approach and use it in following subsections to understand the Monte Carlo results.

A. TPSC approach

The TPSC approach[16,31] can be summarized as follows. One approximates spin and charge susceptibilities $\chi_{\rm sp}$, $\chi_{\rm ch}$ by RPA-like forms but with two different effective interactions $U_{\rm sp}$ and $U_{\rm ch}$ which are then determined self-consistently. Although the susceptibilities have an RPA functional form, the physical properties of the theory are very different from RPA because of the self-consistency conditions on $U_{\rm sp}$ and $U_{\rm ch}$. The necessity to have two different effective interactions for spin and for charge is dictated by the Pauli exclusion principle $\langle n_\sigma^2\rangle=\langle n_\sigma\rangle$ which implies that both $\chi_{\rm sp}$ and $\chi_{\rm ch}$ are related to only one local pair correlation function $\langle n_\uparrow n_\downarrow\rangle$. Indeed, using the fluctuation-dissipation theorem in Matsubara formalism and the Pauli principle one can write

$$\frac{1}{\beta N}\sum_q \chi_{\rm ch}(q)=n+2\langle n_\uparrow n_\downarrow\rangle-n^2 =\frac{1}{\beta N}\sum_q \frac{\chi_0(q)}{1+\frac{1}{2}U_{\rm ch}\chi_0(q)}, \quad (4)$$

$$\frac{1}{\beta N}\sum_q \chi_{\rm sp}(q)=n-2\langle n_\uparrow n_\downarrow\rangle=\frac{1}{\beta N}\sum_q \frac{\chi_0(q)}{1-\frac{1}{2}U_{\rm sp}\chi_0(q)}, \quad (5)$$

where $\beta\equiv 1/T$, $n=\langle n_\uparrow\rangle+\langle n_\downarrow\rangle$, $q=(\mathbf{q},iq_n)$ with $\mathbf{q}$ the wave vectors of an N site lattice, iq_n Matsubara frequencies, and $\chi_0(q)$ the susceptibility for noninteracting electrons. The first equalities in each of the above equations are an exact sum rule, while the last equalities define the TPSC approximation for $\chi_{\rm ch}(q)$ and for $\chi_{\rm sp}(q)$. In this approach, the value of $\langle n_\uparrow n_\downarrow\rangle$ may be obtained self-consistently[16] by adding to the above set of equations the relation $U_{\rm sp}=g_{\uparrow\downarrow}(0)U$ with $g_{\uparrow\downarrow}(0)\equiv\langle n_\uparrow n_\downarrow\rangle/\langle n_\downarrow\rangle\langle n_\uparrow\rangle$. As shown in Ref. 16, the above procedure reproduces both Kanamori-Brueckner screening as well as the effect of Mermin-Wagner thermal fluctuations, giving a phase transition only at zero-temperature in two dimensions. In general, there is, however, a crossover temperature T_X below which the magnetic correlation length ξ grows exponentially. Quantitative agreement with Monte Carlo simulations is obtained[16] for all fillings and temperatures in the weak to intermediate coupling regime $U<8$. The equation for charge Eq. (4) is not necessary to obtain the spin structure factor discussed below.

B. Numerical results and interpretation of the maximum in the uniform magnetic susceptibility

As above, at $\mathbf{q}=0$ the magnetic structure factor is related by the fluctuation-dissipation theorem to the uniform magnetic susceptibility, $\chi\equiv\chi_{\rm sp}(q=0)$ which can be measured either directly[32] or through NMR Knight shift. One of the puzzling aspects of this quantity in high-temperature superconductors is the doping dependence of its extrapolated zero-temperature value. It increases with doping before decreasing again for larger dopings.

The uniform magnetic susceptibility χ that we obtain numerically is plotted as a function of filling in Fig. 2 for the nearest-neighbor model (hopping parameter t) (Refs. 33 and 34) and in Fig. 3 for the model where next-nearest-neighbor hopping (hopping parameter t') is allowed. Recalling that filling $\langle n\rangle$, that measures the average number of electrons per site, is equal to one minus doping, the experimentally observed maximum is qualitatively described by both models. The physical origin of both results is however very different. In the $t'=0$ model, Fig. 2, the maximum comes purely from the interactions since the $U=0$ model does not have a maximum as a function of doping. By contrast, the model $t'\neq 0$ in Fig. 3 has a maximum even at $U=0$ (dashed-dotted line). This maximum is simply enhanced by interactions, as we now discuss.

In the $t'\neq 0$ case, Fig. 3, the magnitude of finite-size effects coming from the thermal de Broglie wavelength can be estimated from the $U=0$ result that is plotted for both 8×8 and infinite lattices. Figures 6(a) and 6(b) show that at all $\mathbf{q}$ the overall agreement is excellent between the TPSC approach[16] and Monte Carlo simulations of the structure factor. The two fillings illustrated correspond to half-filling and to a filling close to the van Hove singularity. We have already commented on the discrepancy for the half-filled case at $\mathbf{q}=(\pi,\pi)$ in the section on finite-size effects. Among other $\mathbf{q}$ points, it is for the $\mathbf{q}=0$ results that the discrepancy with the TPSC is largest, as in Fig. 3. Given the difference in scale between the results at $\mathbf{q}=0$ and $\mathbf{q}=(\pi,\pi)$, it is understandable that the $\mathbf{q}=0$ result is less precise because in TPSC it is only the integral over all $\mathbf{q}$ that is determined self-consistently. Finite-size analysis of the $U=0$ case and TPSC itself (finite mesh calculation) suggests that Monte Carlo calculations on 10×10 would suffice to completely eliminate finite-size effects. The TPSC then allows us to conclude that the physical origin of the maximum in χ as a function of

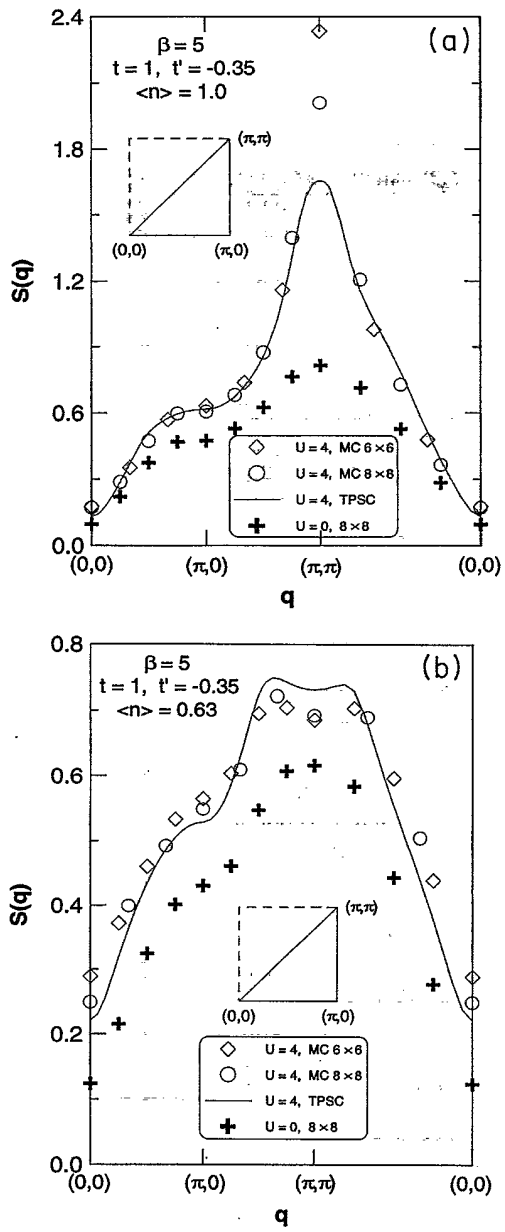

FIG. 6. Magnetic structure factor measured along the sides of the irreducible Brillouin zone illustrated in the insets. The TPSC calculation is for the infinite lattice. (a) Half-filled case (b). Filling near the van Hove singularity.

filling for the $t'=-0.35$ model in Fig. 3 is a band-structure effect (van Hove singularity) which is already present for the noninteracting system ($U=0$) and only enhanced by interactions. No complication in the interpretation can arise from antiferromagnetism since, as discussed in the section on finite-size effects, it does not occur in this $t'=-0.35$, $U=4$ model.

By contrast, in the $t'=0$ model of Fig. 2 the mechanism by which interactions create the maximum is not so clear. A phenomenological interpretation in weak coupling has been *proposed*.[35] However, the TPSC approach does not show a maximum nor does the slave-boson approach[36] for this value $U=4$. This qualitative disagreement strongly suggests that the maximum is a self-energy effect (appearance of a pseudogap). This self-energy effect is important in strong coupling where both slave bosons[36] and numerical simulations[33] do show a maximum. It can also be important in the presence of strong antiferromagnetic fluctuations even at relatively weak coupling $U=4$ but it is not included in the present version of either the TPSC approach or slave bosons. However, one can show that the self-energy obtained at the next level of approximation in a manner consistent with the TPSC approach does show a pseudogap.[31] This pseudogap appears as soon as the antiferromagnetic correlation length becomes larger than the thermal de Broglie wavelength $\xi_{\rm th}$. The pseudogap is more pronounced at half-filling, leading to a relative decrease of the density of states, and correspondingly of the magnetic susceptibility. This is what might explain the maximum away from half-filling: As one increases the electronic density towards half-filling, the magnetic susceptibility increases because of the increase in density of states until the presence of antiferromagnetic fluctuations creates a pseudogap that depletes the density of states more and more as we move towards half-filling.

Finite-size effects on the pseudogap are negligible as long as $\xi_{\rm th}$ is smaller than the system size, even when the antiferromagnetic correlation length is larger than system size.[31] The TPSC as well as numerical simulations at $\mathbf{q}=(\pi,\pi)$ do show that, for the parameters of Fig. 2, we are precisely in this situation, namely the antiferromagnetic correlation length is larger than $\xi_{\rm th}$ but $\xi_{\rm th}$ is less than or of the order of the system size.[38–40] Hence the apparent convergence of the Monte Carlo results as a function of system size, despite the large antiferromagnetic correlation length, would be consistent with the above self-energy (pseudogap) interpretation of the maximum.

C. Antiferromagnetic correlations vs zero-temperature phase diagram

Recently, Duffy and Moreo[12] have found antiferromagnetism for the $t'=-0.2$ model at half-filling for both $U=4$, $\beta=6$, and $U=6$, $\beta=4$. They also found that antiferromagnetism disappears away from half-filling. This seems in contradiction with the zero-temperature phase diagram[14] which predicts that antiferromagnetism would be favored near the filling corresponding to the van Hove singularity that is here at finite hole doping. We checked that the TPSC approach accurately reproduces the results of Duffy and Moreo[12] and allows us to understand their origin. The crossover to a regime where in two dimensions the antiferromagnetic correlation length starts to grow exponentially[16] occurs at a temperature T_X that is comparable with t', hence the details in the band structure introduced by t' are not crucial and antiferromagnetism appears first at $n=1$, as in the $t'=0$ case. Note that even in this $t'=0$ case, the TPSC predicts[16] that slightly away from half-filling the crossover to a rapidly growing correlation length occurs at the antiferromagnetic wave vector, not at an incommensurate wave vector, again in apparent contradiction with the zero-temperature phase diagram. The key point in all this is that the shape and position of the maximum in $\chi_{\rm sp}(\mathbf{q},iq_n=0)$ at $T=T_X$ can be qualitatively different from that at $T=0$. This shows that it is a misconception to believe that the zero-temperature phase

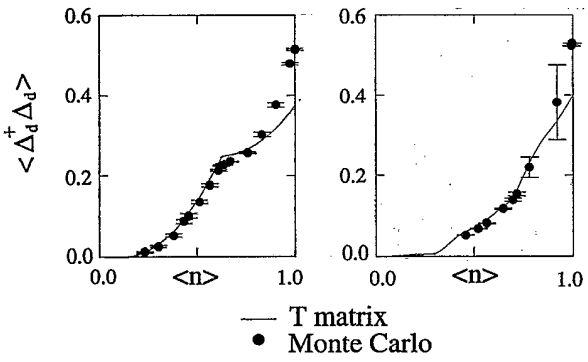

FIG. 7. Reproduced from Fig. 6 of Ref. 17. Singlet d-wave correlation function plotted as a function of filling in the nearest-neighbor ($t'=0$) model for $U=4$, $\beta=6$. The T-matrix result is the same as the $U=0$ result and is calculated on the same lattice sizes at the same temperature $\beta=6$. (a) 4×4 lattice; (b) 8×8 lattice.

diagram determines the high-temperature finite-size calculations, or even the real three-dimensional finite-temperature phase transition. In fact whether the finite-temperature phase transition is commensurate *or* incommensurate may be predicted in a more realistic manner from TPSC or finite-size scaling at finite temperature rather than from zero-temperature calculations. For example, two-dimensional systems do not show a real phase transition until zero temperature. Nevertheless, if finite-size calculations reveal that the antiferromagnetic correlation length starts to grow with system size at T_X, then in real systems small three-dimensional effects would generally lead to long-range order at the wave vector at which the two-dimensional χ_{sp} has a maximum.[18,19] In the $t'=0$ case slightly away from half-filling this would be at the antiferromagnetic wave vector, not at the incommensurate one.

IV. SUPERCONDUCTING CORRELATIONS AND T-MATRIX EFFECTS

The order parameter for superconductivity is defined by

$$\Delta_\alpha^\dagger \equiv \sum_i \Delta_\alpha^\dagger(\mathbf{r}_i) \equiv \frac{1}{2\sqrt{N}} \sum_{i,\nu} g^\alpha(\nu) c_{i,\uparrow}^\dagger c_{i+\nu,\downarrow}^\dagger , \qquad (6)$$

where the sum over ν is over the nearest-neighbor sites of i. The form factor determines the spatial symmetry (s, extended S,p,d) of the Cooper pair.[37] For singlet order parameters the form factor is even in space $g^\alpha(\nu)=g^\alpha(-\nu)$, and the spatial symmetries usually considered include

$$s \text{ wave, with } g^\alpha(\nu)=\delta_{\nu,0}, \qquad (7)$$

$$\text{extended } S \text{ wave, with } g^\alpha(\nu)=\delta_{\nu,\mathrm{x}}+\delta_{\nu,-\mathrm{x}}+\delta_{\nu,\mathrm{y}}+\delta_{\nu,-\mathrm{y}}, \qquad (8)$$

$$d \text{ wave, with } g^\alpha(\nu)=\delta_{\nu,\mathrm{x}}+\delta_{\nu,-\mathrm{x}}-\delta_{\nu,\mathrm{y}}-\delta_{\nu,-\mathrm{y}}. \qquad (9)$$

For the nearest-neighbor model ($t'=0$), we have shown in an earlier paper[17] that most of the correlations at low density can be accounted for by two-body particle-particle scattering, namely T-matrix effects. Near half-filling, one observes deviations from T-matrix predictions, especially for

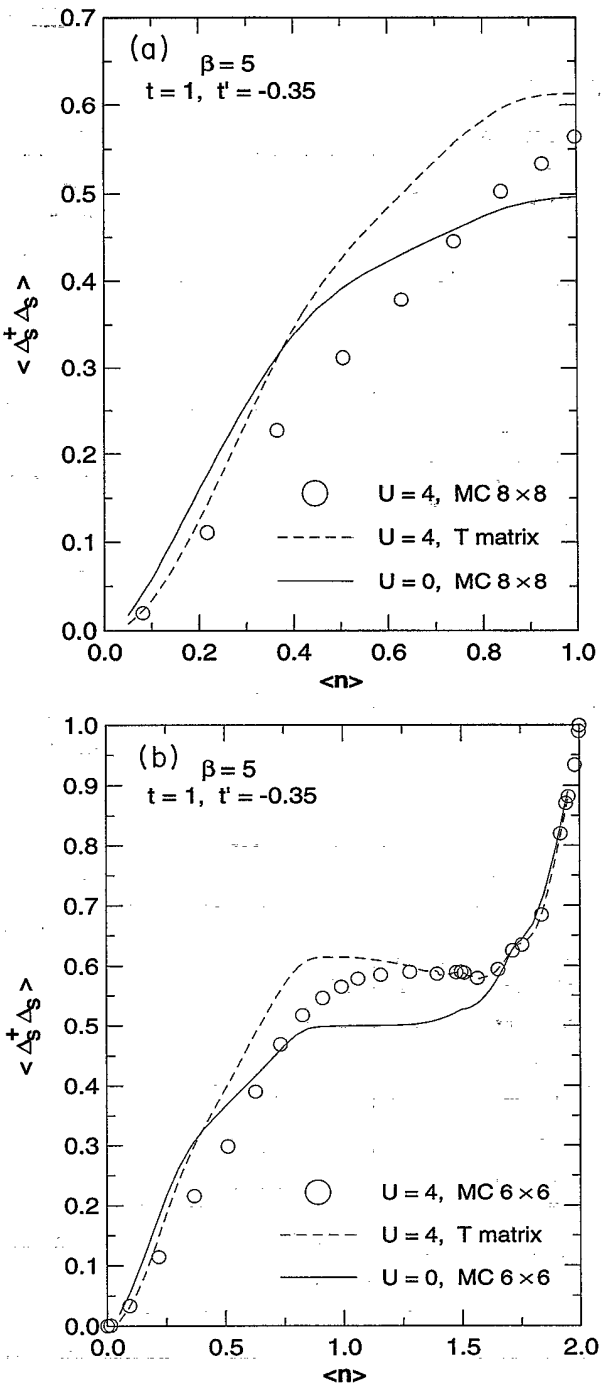

FIG. 8. Order parameter correlations for extended S-wave superconductivity. (a) 8×8 system for $\langle n\rangle\leq1$; (b) 6×6 system for the whole range of fillings.

the d-wave correlations. Figure 7, reproduced from Ref. 17, shows that the T matrix underestimates superconducting fluctuations at half-filling. Since for d wave the T matrix gives in fact the same result as the noninteracting case,[17,18] this means that the correlations measured by Monte Carlo simulations are enhanced compared with the noninteracting case. This could indicate that either the van Hove singularity or the nesting-induced antiferromagnetism increase d-wave correlations.

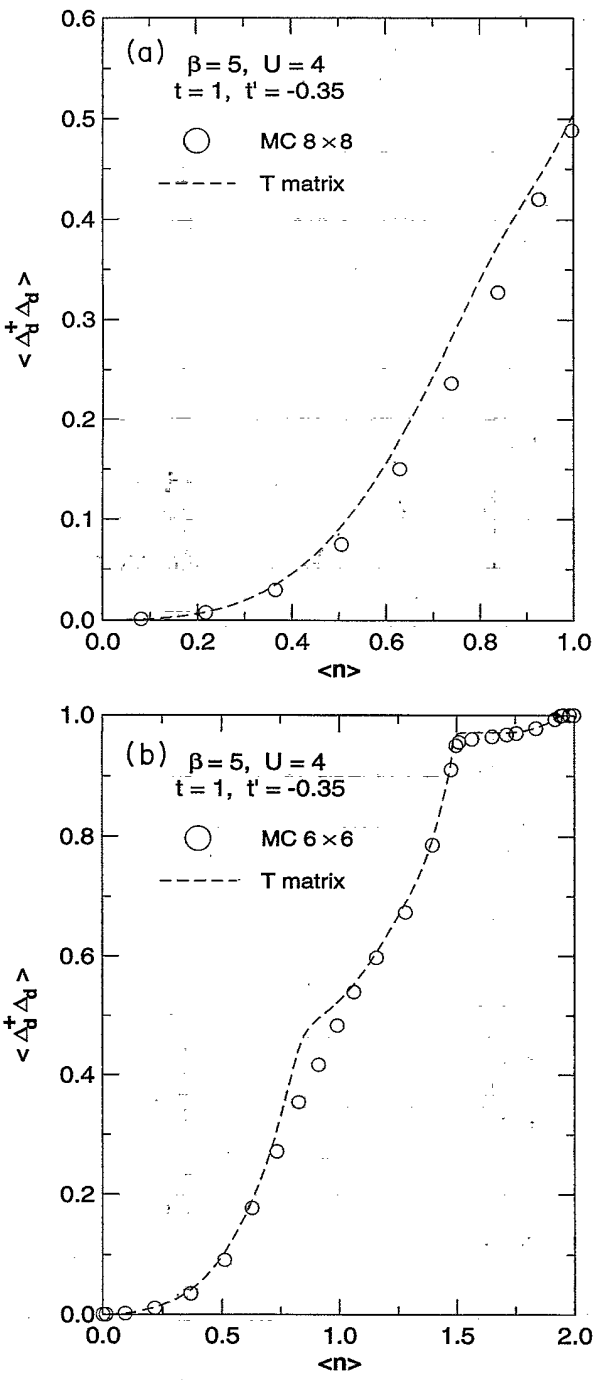

FIG. 9. Order parameter correlations for d-wave superconductivity. (a) 8×8 system for $\langle n\rangle\leq 1$; (b) 6×6 system for the whole range of fillings.

The $t'=-0.35$ Monte Carlo results in Figs. 8 and 9 can help disentangle the influence of van Hove singularity and nesting. It is apparent from the figures, however, that size effects are still quite large. At this temperature, we cannot really expect results that would converge to the infinite size limit before 10×10 lattices. To account for this, the calculations for the T matrix are done for systems of the same size as the Monte Carlo simulations, as has been done in the $t'=0$ model.[17] From Figs. 8 and 9, we learn that (a) as expected in general and as found in particular in the $t'=0$ case, the T-matrix approximation works best at low electron or hole filling, i.e., near $\langle n\rangle=0$ and $\langle n\rangle=2$. (b) The disagreement between simulations and T matrix is largest on the $\langle n\rangle<1$ side in the vicinity of the van Hove singularity. (c) The T matrix everywhere overestimates the superconducting correlations. Even though this should in no way be considered a proof, this last point suggests that the finite t' model is even less favorable to superconductivity than the nearest-neighbor model. Earlier studies,[6,8–10] are equally divided on this point. Here, no sign of superconductivity is found in the size dependence of correlations functions. A plot of the spatial dependence[6,10] would, however, be a more sensitive test.

As mentioned in the context of the magnetic structure factor, the parameters studied here do not correspond to a regime where antiferromagnetism has started to set in at half-filling, contrary to the studies of the $t'=0$ model. For the $t'=0$ model the only case where the T matrix clearly underestimates the superconducting correlations is for d-wave pairing near half-filling[17,18] at a temperature where nesting and antiferromagnetic correlations are strong. Since the van Hove singularity located at the same filling is expected to decrease pairing correlations, as in remark (b) above, this seems a clear indication that antiferromagnetism increases superconducting fluctuations. We have not found, however, yet that the increase is sufficient to lead to a superconducting phase transition. To confirm the positive influence of antiferromagnetism on superconductivity, it would be interesting in the $t'\neq0$ case to either increase U or decrease temperature to reach a regime where antiferromagnetism starts to show up in the model. One should beware, however, that antiferromagnetic correlations can have a positive influence on superconducting fluctuations due simply to a short-range effect, as argued in Ref. 41.

V. CONCLUSION

We have studied the next-nearest-neighbor Hubbard model for $t'=-0.35$ and $t'=0$ using both Monte Carlo simulations and analytical approaches. We have also discussed at length finite-size effects. The TPSC approach[16] allowed us to understand the magnetic fluctuation properties, including the occurence of antiferromagnetism observed in previous calculations at half-filling.[12]

The uniform magnetic susceptibility obtained with the $t'=-0.35$ model has the same qualitative doping dependence as the experimental results on high-temperature superconductors. Since we have found that the TPSC approach gives a satisfactory explanation of the spin-spin correlation functions computed by Monte Carlo simulations, we were able to identify the maximum in the magnetic susceptibility as mostly a band-structure effect enhanced by interactions. We contrasted this with the $t'=0$ model where a maximum also shows up but for apparently very different reasons related probably to self-energy (pseudogap) effects which can occur either at strong coupling or in the presence of large antiferromagnetic correlation lengths.

For the interaction and temperature ranges studied here, superconductivity is less favored for $t'=-0.35$ than for the $t'=0$ model since the Monte Carlo results are consistently smaller than trivial T-matrix effects. However, antiferromag-

netic correlations do not occur in this parameter range. It is interesting to note that despite the fact the T matrix *overestimates* superconducting correlations in the presence of a van Hove singularity, in the $t'=0$ case the presence of nesting and concomitant large antiferromagnetic correlations at half-filling suffice to overcome the detrimental effect of the van Hove singularity to increase the superconducting d-wave fluctuations *above* the T-matrix prediction. This clearly suggests that antiferromagnetic correlations can have a positive influence on d-wave pairing. However, the effect observed to date is clearly a short-range one so that the issue of long-range superconducting order caused by antiferromagnetic correlations is not settled yet.

ACKNOWLEDGMENTS

We acknowledge the support of the Natural Sciences and Engineering Research Council of Canada (NSERC), the Fonds pour la formation de chercheurs et l'aide à la recherche from the Government of Québec (FCAR) and (A.-M.S.T.), the Canadian Institute for Advanced Research (CIAR), and the Killam foundation. A.V. would like to thank the Fujitsu corporation for support.

[1] J. Phys. Chem. Solids **54**, 1073 (1993).
[2] K. Levin *et al.*, Physica C **175**, 449 (1991); J. Phys. Chem. Solids **52**, 1337 (1991); Qimiao Si, Y. Zha, K. Levin, and J.P. Lu, Phys. Rev. B **47**, 9055 (1993).
[3] P.B. Littlewood, J. Zaanen, G. Aeppli, and H. Monien, Phys. Rev. B **48**, 487 (1993).
[4] M. Lavagna and G. Stemmann, Phys. Rev. B **49**, 4235 (1994).
[5] Pierre Bénard, Liang Chen, and A.-M.S. Tremblay, Phys. Rev. B **47**, 15 217 (1993).
[6] A. Moreo and D.J. Scalapino, Phys. Rev. B **43**, 8211 (1991).
[7] H.Q. Lin and J.E. Hirsch, Phys. Rev. B **35**, 3359 (1987).
[8] H.Q. Lin, J.E. Hirsch, and D.J. Scalapino, Phys. Rev. B **37**, 7359 (1988).
[9] R.R. dos Santos, Phys. Rev. B **39**, 7259 (1989).
[10] T. Husslein, I. Morgenstern, D.M. Newns, P.C. Pattnaik, J.M. Singer, and H.G. Matuttis (unpublished).
[11] N. Furukawa and M. Imada, J. Phys. Soc. Jpn. **61**, 3331 (1992).
[12] Daniel Duffy and Adriana Moreo (unpublished).
[13] Preliminary accounts of this work have appeared in Alain F. Veilleux, Anne-Marie Daré, Liang Chen, Y.M.Vilk, and A.-M.S. Tremblay, in *Proceedings of Supercomputing Symposium 1994*, June 1994, edited by John W. Ross (University of Toronto Press, Toronto, 1994), p. 78 and in A. Veilleux, M.Sc. thesis, Université de Sherbrooke, 1994.
[14] A zero-temperature RPA phase diagram for the $t'\neq 0$ model appears in Pierre Bénard, Ph.D. thesis, Université de Sherbrooke, 1993.
[15] "Analytical" approaches such as perturbation theory, T-matrix, or TPSC approach, in general need the help of numerical integrations. Nevertheless, we call these approaches "analytical" in the sense that their approximations and physical interpretation follow from analytical arguments, even though their quantitative numerical predictions can generally be found only with the help of a computer.
[16] Y.M. Vilk, Liang Chen, and A.-M.S. Tremblay, Phys. Rev. B **49**, 13 267 (1994).
[17] Anne-Marie Daré, Liang Chen, and A.-M.S. Tremblay, Phys. Rev. B **49**, 4106 (1994).
[18] A.-M. Daré, Ph.D. thesis, Université de Sherbrooke, 1994.
[19] Anne-Marie Daré, Y.M. Vilk, and A.-M.S. Tremblay (unpublished).
[20] J.E. Hirsch, Phys. Rev. B **31**, 4403 (1985).
[21] R. Blankenbecler, D.J. Scalapino, and R.L. Sugar, Phys. Rev. D **24**, 2278 (1981).
[22] For a review see E.Y. Loh and J.E. Gubernatis, in *Electron Phase Transitions*, edited by W. Hanke and Y.V. Kopaev (Elsevier, Amsterdam, 1992), pp. 177–235. Also, A.-M.S. Tremblay (unpublished).
[23] S.R. White, D.J. Scalapino, R.L. Sugar, E.Y. Loh, J.E. Gubernatis, and R.T. Scalettar, Phys. Rev. B **40**, 506 (1989).
[24] Liang Chen and A.-M.S. Tremblay, Int. J. Mod. Phys. B **6**, 547 (1992).
[25] J.E. Hirsch, Phys. Rev. B **31**, 4403 (1985).
[26] M.S. Hybertsen, E.B. Stechel, W.M.C. Foulkes, and M. Schluter, Phys. Rev. B **45**, 10 032 (1992).
[27] W.E. Pickett, R.E. Cohen, and H. Krakauer, Phys. Rev. B **42**, 8764 (1990).
[28] N.E. Bickers and S.R. White, Phys. Rev. B **43**, 8044 (1991).
[29] Liang Chen, C. Bourbonnais, T. Li, and A.-M.S. Tremblay, Phys. Rev. Lett. **66**, 369 (1991).
[30] N. Bulut, D.J. Scalapino, and S.R. White, Phys. Rev. B **47**, 2742 (1993).
[31] Y.M. Vilk and A.-M.S. Tremblay (unpublished).
[32] J.B. Torrance, A. Bezinge, A.I. Nazzal, T.C. Huang, S.S.P. Parkin, D.T. Keane, S.J. Laplaca, P.M. Horn, and G.A. Held, Phys. Rev. B **40**, 8872 (1989).
[33] A. Moreo, Phys. Rev. B **48**, 3380 (1993).
[34] Liang Chen and A.-M.S. Tremblay, Phys. Rev. B **49**, 4338 (1994).
[35] Thilo Kopp and Frédéric Mila, Phys. Rev. B **50**, 13 017 (1994).
[36] R. Frésard and K. Doll, in NATO Workshop, *The Physics and the Mathematical Physics of the Hubbard Model* (San Sebastian, 1993), edited by D. Campbell, D. Baeriswil, P. Guinea, and E. Verges (Plenum, New York, 1995).
[37] For a discussion of order-parameter symmetries in high temperature superconductors, see Liang Chen and A.-M.S. Tremblay, J. Phys. Chem. Solids **54**, 1381 (1993) and C.M. Varma (unpublished).
[38] In the three-band model, Dopf *et al.* (Ref. 39) have found a parameter range where the behavior observed experimentally is reproduced qualitatively and it seems that, in this parameter range, strong antiferromagnetic correlations are also present at half-filling (Ref. 40).
[39] G. Dopf, A. Muramatsu, and W. Hanke, Phys. Rev. Lett. **68**, 353 (1992). See Fig. 3 of this paper.
[40] G. Dopf, A. Muramatsu, and W. Hanke, Phys. Rev. B **41**, 9264 (1990). See Fig. 8 of this paper.
[41] D.J. Scalapino, in *Perspectives in Many-Particle Physics*, edited by R.A. Broglia, J.R. Schrieffer, and P.F. Bortignon (North-Holland, Amsterdam, 1994), pp. 95–125.